[Title Page]

Optimizing the 'Lift-up' Design to Maximize Pedestrian Wind and Thermal Comfort in 'Hot-Calm' and 'Cold-Windy' Climates

A. U. Weerasuriya[a,b], Xuelin Zhang[b]*, Bin Lu[c], Tim K.T. Tse[b], Chun-Ho Liu[a]

[a] *Department of Mechanical Engineering, The University of Hong Kong, Pokfulam, Hong Kong.*

[b] *Department of Civil and Environmental Engineering, The Hong Kong University of Science and Technology, Clear Water Bay, Kowloon, Hong Kong.*

[c] *Department of Architecture and Civil Engineering, City University of Hong Kong, Kowloon Tong, Hong Kong*

*Corresponding author:

Xuelin Zhang

Email: xzhangbn@connect.ust.hk; Tel.: (852) 5519 7725.

Mailing address: Department of Civil and Environmental Engineering,

The Hong Kong University of Science and Technology, Clear Water Bay,

Kowloon, Hong Kong, China

ABSTRACT

A novel building design — the lift-up design — has shown promise in removing obstacles and facilitating wind circulation at lower heights in built-up areas, yet little is understood about how their design parameters can influence the surrounding wind environment. This study develops a framework to study these parameters, and, using the knowledge, to modify the lift-up design to improve both the wind and thermal environments for pedestrians. The framework combines an Artificial Neural Network (ANN)-based surrogate model, an optimization algorithm (Genetic Algorithm), and Computational Fluid Dynamics (CFD) simulation to find the best lift-up design that simultaneously maximizes both pedestrian wind and thermal comfort. The optimization is done for two diametrically different climates: a hot climate with calm wind conditions ('hot-calm'), and a cold climate with windy conditions ('cold-windy'). By adjusting eight parameters, the proposed framework enlarges, by more than 46% and 37% for 'hot-calm' and 'cold-windy' climates respectively, the area near a lift-up building where there is pedestrian wind comfort, and by 18% and 10% respectively for the two climates, the area where there is thermal comfort. These results indicate that optimum lift-up designs strongly depend on how the objective function of the optimization is set: e.g., whether to maximize area with pedestrian wind comfort, or with thermal comfort, or both.

***Keywords*:** Lift-up building; Pedestrian-level wind environment; Genetic Algorithm, Artificial Neural Network; Computational Fluid Dynamics simulation

1. INTRODUCTION

Steadily growing urban populations result in ever-increasing demand for housing and infrastructural facilities. To meet this demand, modern cities have come to have high densities: buildings are tall and closely spaced to fully utilize limited land. Hong Kong, for instance, is archetypically a high-density, compact city — about 12.2% out of 24.9% of its habitable land is covered with buildings, with a high plot ratio (i.e., total gross floor area (GFA) of a building on a site divided by the total site area) of 10 to 8 [1]. Although high-density, compact cities are a highly efficient way of using land and managing public transport, their congested building arrangements cause serious environmental issues and compromise the urban quality of life.

One such environmental issue is weak wind circulation near the ground level, which is a combined result of adverse meteorological conditions and overly dense urban planning ([2], [3], [4]). Weak wind circulation raises many environmental issues; for instance, in Hong Kong, it has worsened outdoor thermal comfort [5], allowed air pollutants to accumulate at the street level [6], amplified the urban heat island effect [7], and created favorable conditions for airborne pathogens to spread [8]. Studies ([3], [9], [10], [11], [12], [13]) have indicated that modifications to urban transformation can improve air movement at the ground level, so many municipal authorities have revised guidelines on building designs in high-density compact cities to resolve urban weak wind circulation and mitigate any negative impact. The Sustainable Building Design (SBD) Guidelines (APP-152) in Hong Kong, for example, have introduced three-building design parameters: building separation, building set back, and site coverage of greenery [14]. Under "building separation", APP-152 recommends a minimum 20% permeability on two projection planes of a building in built-up areas to facilitate wind circulation. One way to provide this level of permeability is to design 'lift-up' buildings (i.e., buildings with a lift-up design).

In the lift-up design, the main structure is elevated from the ground and is supported either by columns, shear walls, center core(s) or a combination of them ([15], [16], [17], [18], [19]). In addition to complying with the permeability guidelines, the lift-up design also maximizes space — by minimizing obstructions — for wind to circulate at lower heights. Moreover, the area underneath the elevated structure, hereafter referred to as "lift-up area", provides space for leisure and recreational activities or access routes. Figure 1 shows two lift-up areas in Hong Kong: the headquarters of the Hongkong and Shanghai Banking Corporation in Central, and a building at the Polytechnic University campus in Hung Hom.

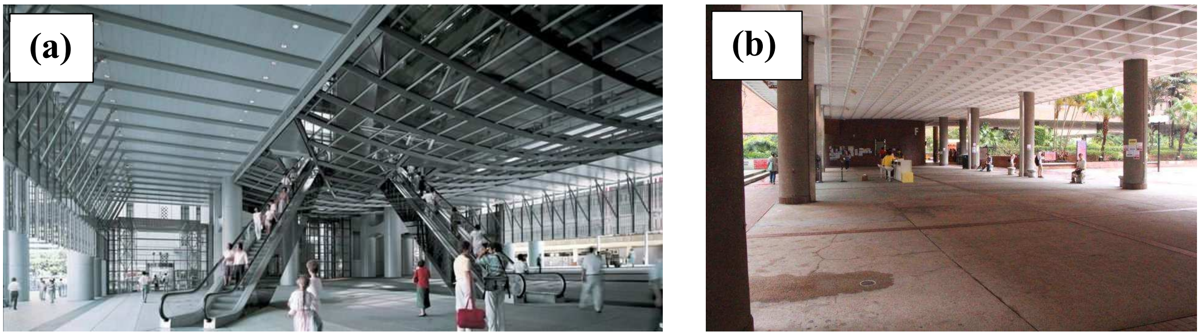

Figure 1. The lift-up area of (a) the headquarters building of Hong Kong and Shanghai Bank (source. http://danielyngblog.com/1931-2/), (b) a campus building in the Polytechnic University of Hong Kong (Photos by Xuelin Zhang).

Lift-up buildings have been shown, using data from the wind tunnel and computational fluid dynamics (CFD) simulations, to be effective in improving wind circulation in their vicinity. Tse et al. [16] and Zhang et al. ([17], [18]) modeled and tested the pedestrian-level wind environment (PLWE) near 29 lift-up building designs (of various dimensions and center core designs) in a boundary layer wind tunnel (BLWT). A series of wind tunnel tests conducted by Xia et al. [15] have indicated that the PLWEs near a single building and near a row of lift-up buildings have better wind circulation than non-lift-up counterparts. By combining data from the wind tunnel and field measurements from a university campus in Hong Kong, Du et al. ([20], [21]) have demonstrated that lift-up designs are effective in creating wind and thermal comfort both inside and near lift-up areas. Moreover, Du et al. [19] and Liu et al. ([22], [23]) employed steady Reynolds Averaged Navier-Stokes (SRANS), Delayed Detached Eddy Simulation (DDES), and Large Eddy Simulation (LES) techniques in CFD simulation to model the pedestrian-level mean and instantaneous wind fields near lift-up buildings. In addition to understanding the PLWE near lift-up buildings, these studies have shed light on important design parameters of the lift-up design. For example, Tse et al. [16] have identified the height of the center core as the most influential parameter and recommend that lift-up designs should start with that parameter, followed by planning the plan area of the center core. Zhang et al. [18] recommend modifying the corners of a center core, as such modification maximizes the area where there are acceptable wind conditions for pedestrians. Du et al. [24] suggest the number of center cores as another important design parameter, perhaps only second to center core aspect ratio (i.e., the ratio between the width and depth of the core).

Although these studies have shed light on the governing lift-up design parameters, they have not guided designers to selecting the best lift-up design — one that creates the best possible wind conditions for pedestrians near the building. In fact, selecting such "best lift-up design" is arduous, as it involves many additional design parameters such as height, width, depth, orientation and shape of both building and core. Zhang et al. [18], using second-order nonlinear regression analysis, have found complex, interdependent, nonlinear relationships between the design parameters and the area with pedestrian wind comfort. Despite this, however, Du et al. [24] have made an attempt — the only one found in the literature — to determine parameters that are most suitable for the lift-up design to create acceptable wind and thermal environments for pedestrians. They have proposed a framework for optimizing the lift-up design by combining DDES simulation, Response Surface Method (RSM), and Genetic Algorithm (GA). In general, their study has indicated the possibility of improving the lift-up design via an optimization process, but, both accuracy and effectiveness of their proposed framework have nevertheless been undermined by several shortcomings: One, only a limited number of design parameters — lift-up height, lift-up core aspect ratio, and lift-up core number — were employed for optimization; others, including dimensions and orientation of the elevated structure, were completely ignored. Two, there were limitations with the RSM method; the RSM method is based on a second-order linear relationship between the three design parameters and the area with wind comfort, therefore cannot precisely stipulate complex, interdependent relationships between the design parameters and wind speeds at the pedestrian level.

The current study aims to eliminate these shortcomings by proposing for the optimization process a framework that has a broad range of design parameters and uses an Artificial Neural Network (ANN)-based surrogate model. The ANN-based surrogate model is more robust than the RSM method, and can establish complex, nonlinear relationships between the design parameters and the surrounding wind environment. As a result, the framework can accommodate more design parameters, including dimensions and orientation of the elevated building and corner modifications of the center core. The framework considers two diametrically different wind and thermal climat 'hot-calm' and 'cold-windy', as opposed to only the single wind and thermal climate considered by Du et al. [24]. Selecting the 'cold-windy' climate is motivated by the fact that lift-up designs are often deemed unfit for cold and windy conditions, as high-speed wind jets often found in lift-up areas can cause wind discomfort and wind chill for pedestrians ([25], [26], [27], [28], [29]).

The framework for optimizing the lift-up design in the two climates is introduced in Section 2, which also describes its major tasks and components including selecting design variables and objective functions, the ANN-based surrogate model, the optimization algorithm and CFD simulation. Section 3 presents various lift-up designs proposed by the optimization, with various wind and thermal conditions considered, and the appropriateness of these lift-up designs assessed via using CFD simulation to model the surrounding PLWE. Section 4 explains some limitations of this study, and Section 5 contains some concluding remarks.

2. FRAMEWORK FOR OPTIMIZING THE LIFT-UP DESIGN

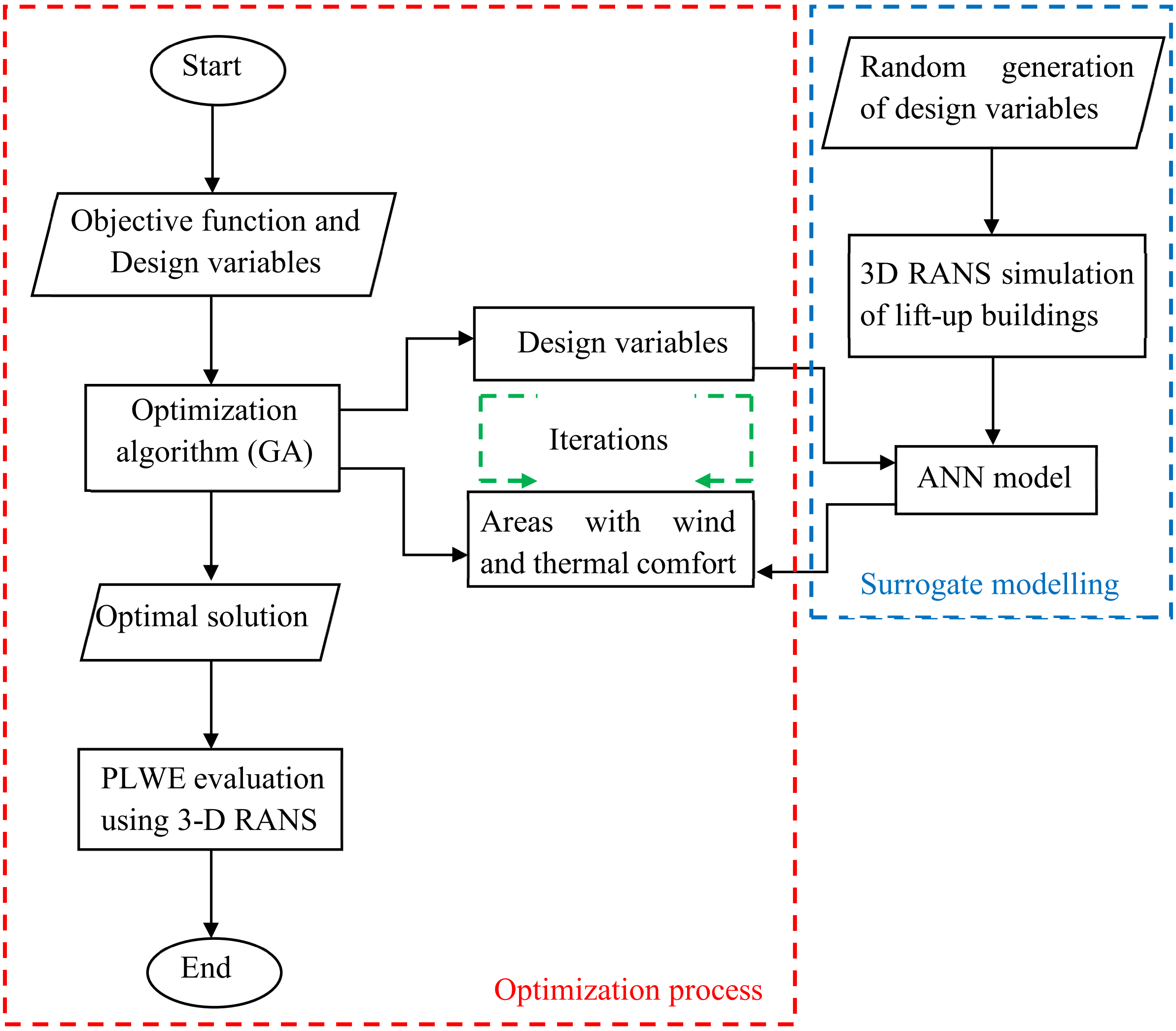

Figure 2. The framework for optimizing the lift-up design

The proposed framework, shown in Figure 2, starts by establishing its objective function as to maximize the area with acceptable pedestrian-level wind and thermal conditions near a lift-up building by searching for the best combination of design variables. Values of the design variables are selected with appropriate upper and lower bounds (constraints) to ensure that the lift-up design is not only realistic but satisfies other architectural and structural considerations. Searching for the best design parameters starts next using a well-known optimization algorithm

— Genetic Algorithm (GA). In a typical searching process, the GA evaluates the objective function corresponding to multiple combinations of the design variables (i.e., candidates) many times (i.e., many generations of candidates). Considering that if such evaluation is based on simulation results (e.g. RANS simulation of PLWE near lift-up buildings) the optimization may be computationally expensive [30], the current study employs an ANN-based surrogate model to evaluate the objective function instead.

A database of the design variables of, as well as the pedestrian-level wind and thermal conditions near 150 lift-up buildings is used to develop the ANN-based surrogate model. The surrogate model is advantageous to the framework because it significantly reduces overall computational costs, speeds up the optimization process as it excludes time-consuming CFD simulations, simplifies the framework by eliminating the direct integration of CFD simulation with the GA, and allows data to be imported from BLWT or CFD simulation to the existing CFD-based database [31]. Owing to their ability to establish complex, nonlinear relationships between inputs and outputs, ANN-based surrogate models are often employed in engineering applications. In wind engineering, ANN-based surrogate models are used to aerodynamically optimize the shapes of tall buildings ([31], [32]), model bridge aerodynamics ([33], [34]), estimate wind pressure on buildings [35], predict building interference effect ([36], [37]), and estimate the wind speed-up effect of topography features [38]. The authors of this paper have previously employed an ANN-based surrogate model to predict the magnitude and direction of wind speeds at the pedestrian level near lift-up buildings [39]; that work has paved the way for the present detailed work. The final step of the framework in this study is to evaluate which combination of design variables gives the optimum lift-up design through comparing, using steady, 3-D RANS simulations, how much the areas where there is pedestrian wind and thermal comfort are enhanced by different optimum and near-optimum designs. The following subsections detail the objective functions, design variables, GA, the 3-D RANS simulation, and the ANN model.

2.1. Objective functions

2.1.1. Climate conditions

The objective functions of this study are set as: to maximize the areas with wind and thermal comfort of pedestrians in two different climates – 'hot-calm', and 'cold-windy'. Wind and thermal comfort are estimated using a set of climate conditions: hourly mean wind speed (*U*), air temperature (T_a), mean radiant temperature (T_{mrt}), and relative humidity (*RH*). This study uses the average conditions of summer in Hong Kong to represent 'hot-calm', and winter in the Netherlands and Sweden for 'cold-windy' climates, as shown in Table 1.

Table 1. Climate conditions in 'hot-calm' and 'cold-windy' climates

Parameter	Magnitude	Reference
'hot-calm' climate		
Wind Speed at 10 m height (*U*)	3.5 ms^{-1}	[40]
Air temperature (T_a)	28°C	[5]
Mean radiant temperature (T_{mrt})	35°C	[41]
Relative Humidity (*RH*)	80%	[5]
'cold-windy' climate		
Wind Speed at 10 m height (*U*)	5 ms^{-1}	[42]
Air temperature	2°C	[43]
Mean radiant temperature	-0.3°C	[43]
Relative Humidity	89%	[43]

2.1.2. Wind comfort criteria

The two wind comfort criteria that this study uses to evaluate PLWE are 'calm' and 'windy' (Table 2). The low ambient wind criterion was proposed by Zhang et al. [18], and the high ambient wind criterion by Lawson [44]. Note that these criteria do not include the maximum allowed probability of exceedance of wind speeds for activity classes, as Zhang et al. [18] have not explicitly defined any threshold probability for their criterion, and a 2% probability for all activity classes has been assumed for Lawson's criterion. Furthermore, this study assumes 1.6-3.5 ms^{-1} and 0-3.6 ms^{-1} mean wind speeds as acceptable wind speeds in the calm and windy climates, respectively.

Table 2: Two wind comfort criteria for clam and windy conditions

Wind Speed (ms^{-1})	Definition /activity	Remarks
Wind comfort criteria for the clam wind climate [18]		
< 1.6	Low wind speed	Cause outdoor thermal discomfort
1.6-3.5	Acceptable wind speeds	Create outdoor thermal comfort
3.5-5	High wind speed	Cause slightly wind discomfort
> 5	Unacceptable wind speeds	Exceed the recommended mean wind speeds in towns [45]
Wind comfort criteria for the windy wind climate [44]		
< 1.8	Pedestrian sitting	Suiable for covered areas
1.8-3.6	Pedestrian standing	Suitable for pedestrian stand around
3.6-5.3	Pedestrian walking	Suitable for pedestrian walk-thru
5.3-7.6	Brisk or fast walking	Acceptable for roads, car parks
>7.6	Unacceptable	Should be avoided from built-up areas

2.1.3. Thermal comfort

Among many popular outdoor thermal comfort indices such as Predicted Mean Vote (PMV) [46], Physiological Equivalent Temperature (PET) [47], and Standard Effective Temperature

(SET*) [48], this study has chosen the recently developed Universal Thermal Climate Index (UTCI) [49]. The UTCI characterizes outdoor thermal comfort by calculating the thermal effects of air temperature; wind speed; direct, diffused and reflected solar radiation; infrared long-wave radiation; and humidity on an average person, then compares it with the air temperature in a reference, uniform environment where the same person would experience the same physiological strain as in the actual environment [50]. As shown in Table 3, the UTCI expresses a number of hot and cold thermal stresses using UTCI equivalent temperature. An online UTCI calculator (http://www.utci.org/utcineu/utcineu.php) is integrated into the framework established in this work and calculates UTCI temperatures in the surrounding of the lift-up buildings. The lowest UTCI ranges found near the 150 lift-up buildings in the two climates were +26 to +32 ºC and 0 to +9 ºC and to maximize areas with these UTCI ranges were selected as the objective functions in 'hot-calm'and 'cold-windy' climates, respectively.

Table 3. UTCI equivalent temperatures categorised in terms of thermal stress [51]

UTCI range (°C)	Stress category
Above +46	Extreme heat stress
+38 to +46	Very strong heat stress
+32 to +38	Strong heat stress
+26 to +32	Moderate heat stress
+9 to +26	No thermal stress
+9 to 0	Slight cold stress
0 to −13	Moderate cold stress
−13 to −27	Strong cold stress
−27 to −40	Very strong cold stress
Below −40	Extreme cold stress

2.2. Design variables

The lift-up design selected for this study is similar to the one previously tested in a BLWT by Tse et al. [16], and Zhang et al. ([17], [18]). The lift-up design has a center core that supports the main structure elevated from the ground as shown in Figure 3. Since the current study aims to determine the best lift-up design for a given building, the dimensions of both main structure and center core are considered as design variables. There are eight design variables: height (*H*), width (*W*) of the main structure, height (*h*), width (*w*), depth (*d*), shape (parameters v_1 and v_2) of the central core, and orientation of the building (θ). v_1 and v_2 are defined as $v_1 = t/d$ and $v_2 = a/t$, and by varying them, different aerodynamic modifications are applied to the center core. Note that the depth of the building (*D*) is considered constant and is 20 m for all lift-up buildings. The selected design variables and their upper and lower bounds are shown in Table 4.

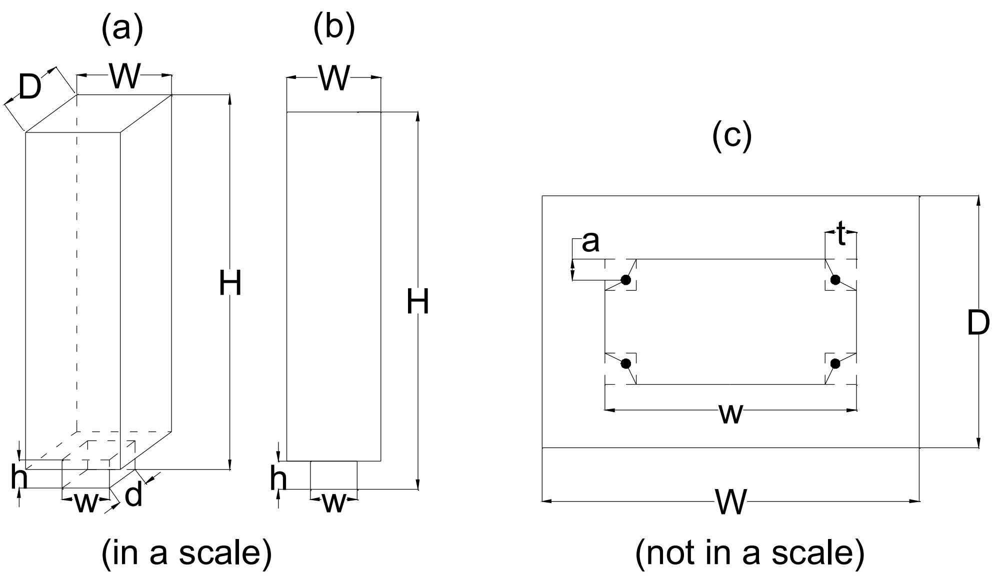

Figure 3. Schematics of a 'lift-up 'building (a) 3-D view, (b) front view, and (c) plan view of center core

Table 4. Design parameters and their upper and lower bounds

	Design parameter	Upper and lower bounds
Building	Height (*H*)	45m < *H* < 120m
	Width (*W*)	30m < *W* < 90m
Central core	Height (*h*)	3m < *h* < 9m
	Width (*w*)	9m < *w* < *W*
	Depth (*d*)	6m < *d* < min (20m, *w*)
	$v_1 = t/d$	$0 < v_1 < 1/3$
	$v_2 = t/a$	$-1 < v_2 < 0$
Orientation	θ	$0^{\circ} < \theta < 45^{\circ}$

2.3.Genetic Algorithm (GA)

As shown in Figure 4, the GA starts with defining objective functions, design variables and their upper and lower bounds, population size and number of generations, and methods of operators. The GA first generates the initial population with 300 candidates whose design variables are expressed as binary codes. Then the GA initiates the search for the best candidates by evaluating the areas with wind and thermal comfort of multiple candidates in the initial population and sorts them according to fitness, i.e., in descending sizes of wind and thermal comfort areas at the PLWE. Two operators, crossover and mutation, are applied to the candidates to generate offspring for the next generation. The crossover operator generates offspring from the candidates (parents) with higher fitness, whereas the mutation operator selects parents with lower fitness to generate offspring. This process ensures that the GA searches a large design space without stagnating into local extreme values, and that it results in local maxima of the objective functions rather than reaching the global maxima. The process continues until no significant improvements in the areas with wind and thermal comfort are observed over generations, or the number of generations has reached the predefined value of 500. The fittest candidate in the last generation is selected as the optimal solution and its design variables represent the best lift-up design, i.e., the one with the largest areas of wind and thermal comfort near the lift-up building.

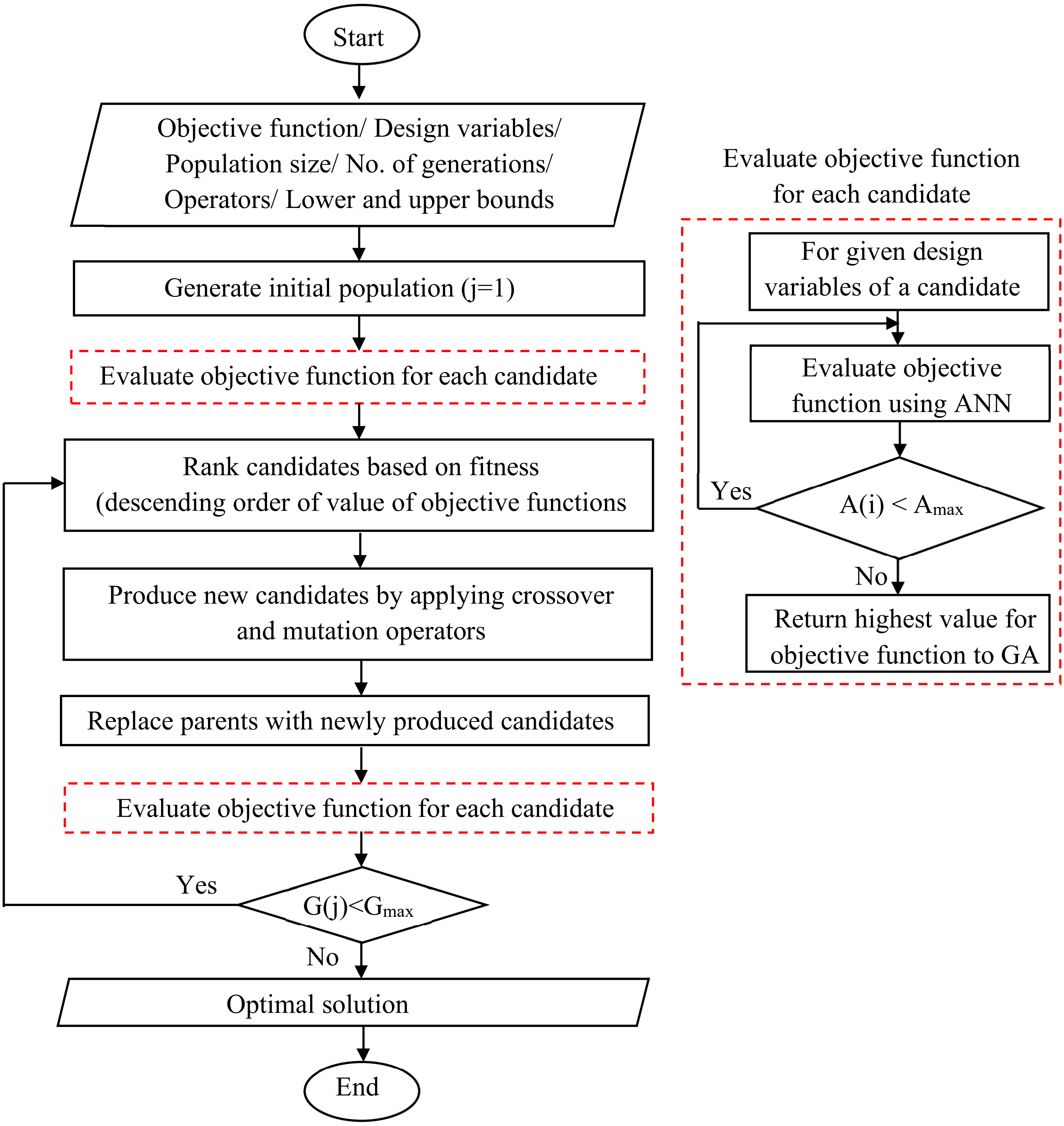

Figure 4. The genetic algorithm (GA) process

2.4.ANN model

The current study used a forward feed, back-propagation ANN model as the surrogate model and it was trained, validated, and tested using a CFD-generated data set that consisted of the design variables and areas with wind and thermal comfort in both‘ hot-calm ’and ‘cold-wind ’ climates. The design variables of the 150 lift-up buildings were randomly selected from a database of 1000 lift-up buildings, whose design variables were randomly generated. This procedure ensured that the magnitudes of the design variables were randomly distributed over the entire range of design space, as shown in Figure 5.

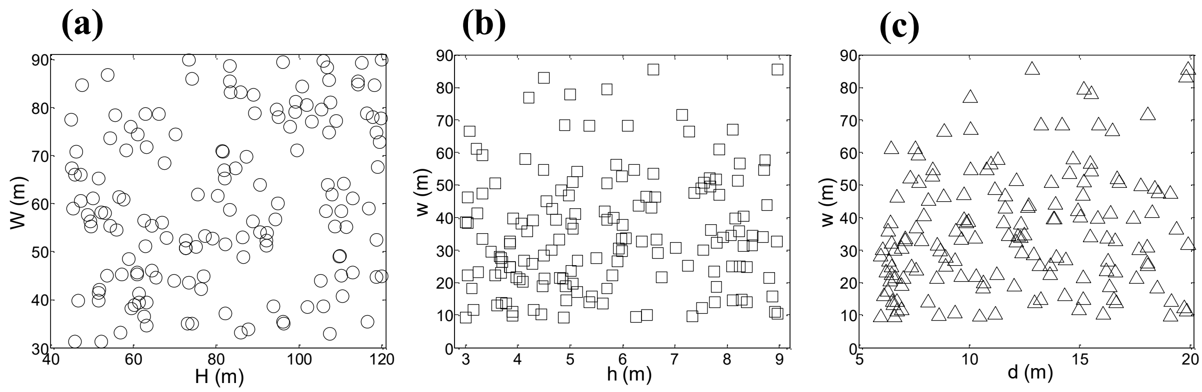

Figure 5. Distribution of (a) building height (*H*) and width (*W*), (b) central core height (*h*) and width (*w*), and (c) center core depth (*d)* and width (*w*)

The ANN model used for this study was a three-layer model: it had an input layer, a hidden layer, and an output layer. The input and output layers had, respectively, eight and two nodes for the eight design variables and the two outputs — the areas of wind comfort and thermal comfort. The areas were expressed as a percentage of the interrogated area of 240 m (width) × 150 m (depth) around the lift-up building (Eq. (1) and (2)), referring to the percentage areas of pedestrian wind comfort (P_{com}) and of thermal comfort (T_{com}).

$$\text{Percentage area of wind comfort } (P_{com}) = \frac{\text{Area with pedestrian wind comfort } (\text{m}^2)}{\text{The interogated area } (\text{m}^2)} \times 100\% \quad (1)$$

$$\text{Percentage area of thermal comfort } (T_{com}) = \frac{\text{Area with thermal comfort } (\text{m}^2)}{\text{The interogated area } (\text{m}^2)} \times 100\% \qquad (2)$$

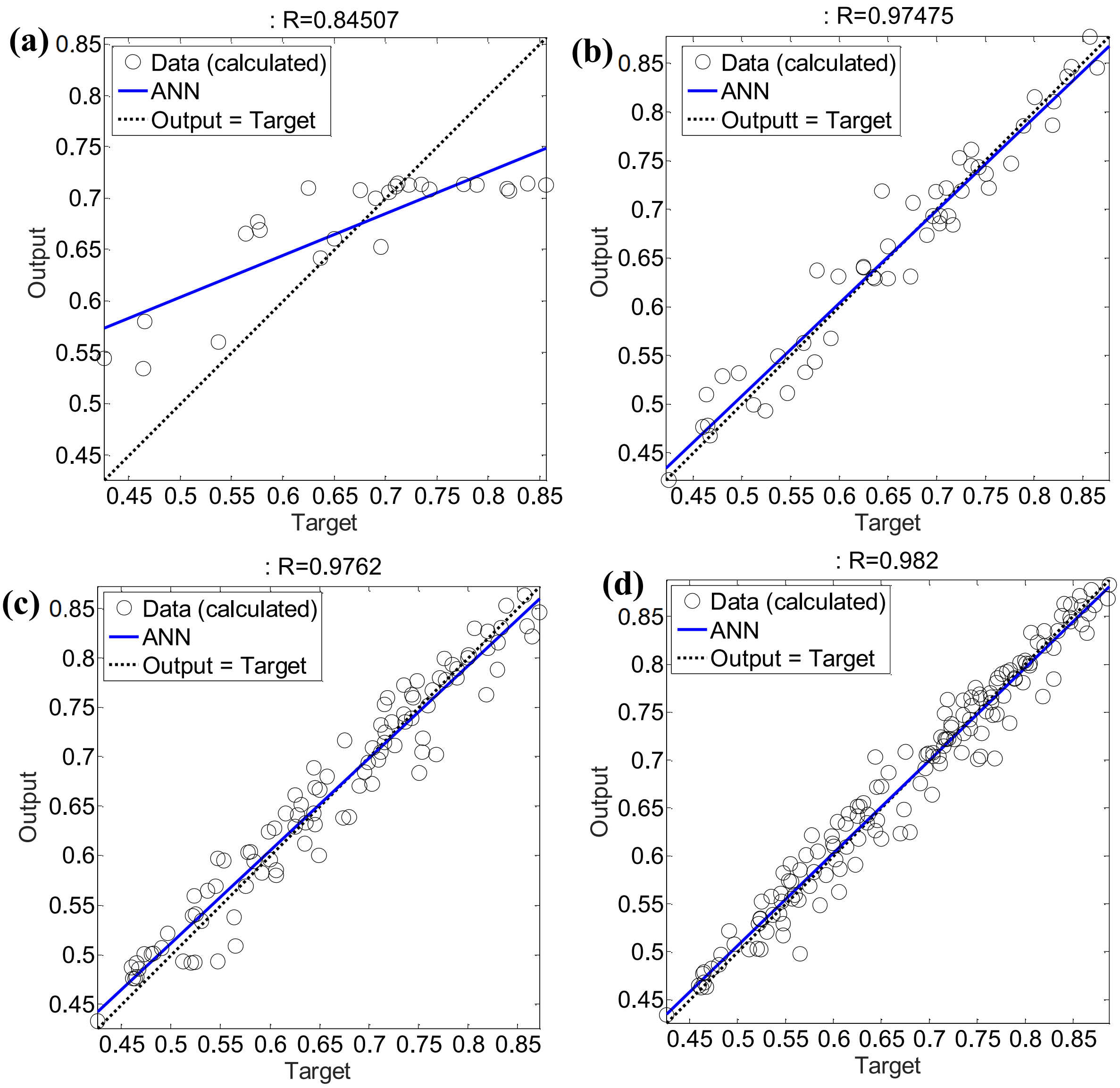

Figure 6. The comparison between ANN prediction of P_{com} and CFD results (a) 25 samples, (b) 50 samples, (c) 100 samples and (d) 149 samples

Many combinations of different numbers of layers and nodes were tested for the hidden layer before one hidden layer with 20 nodes was assigned to the ANN model. In addition, different sizes of data samples were used for training the ANN model (Figure 6), and, finally, 125 data were selected for training the ANN model and the remaining 25 data for validation (i.e., a total of 150 data). This combination yielded a good accuracy in predicting P_{com} and T_{com}, as can be seen in the error distribution in Figure 7(a), where more than 84% of the predictions had 4% or less discrepancy and a high correlation coefficient (R) = 0.982 between the ANN predictions and CFD results (Figure 7(b)).

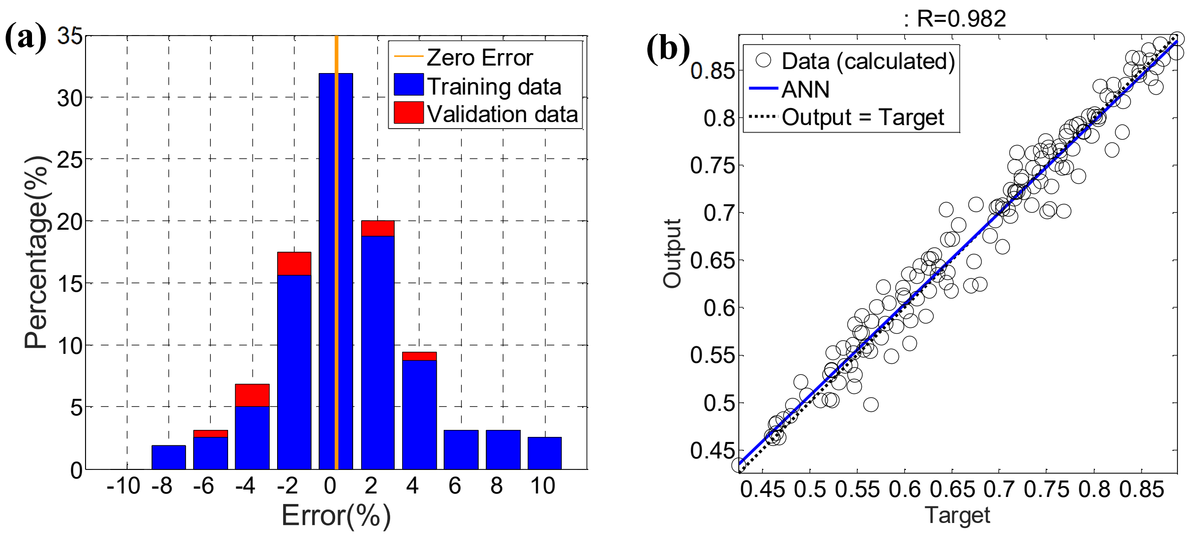

Figure 7. (a) Error distribution of ANN predictions and (b) the comparison between ANN prediction and CFD results for 150 buildings

2.5. CFD simulation

The CFD simulation of this study was carried out using the commercial software package ANSYS FLUENT 15.1. The CFD simulation began with creating the geometries of the lift-up buildings according to the selected design variables and converting them into Standard ACIS Text (SAT) file format, which is readable by FLUENT. The FLUENT meshing tool was employed to create a computational domain where the inlet was 1800 mm (3H) upstream, the outlet was 6000 mm (10H) downstream, the top was 1800 mm (3H) above, and the lateral sides were 1800 mm (3H) away from the building according to the recommendation of the AIJ best practice guidelines [52] (Figure 8a). The computation domain was subsequently discretized into small hexahedral cells and five layers of prisms were created above the ground to the pedestrian level height of 2 m (Figure 8b).

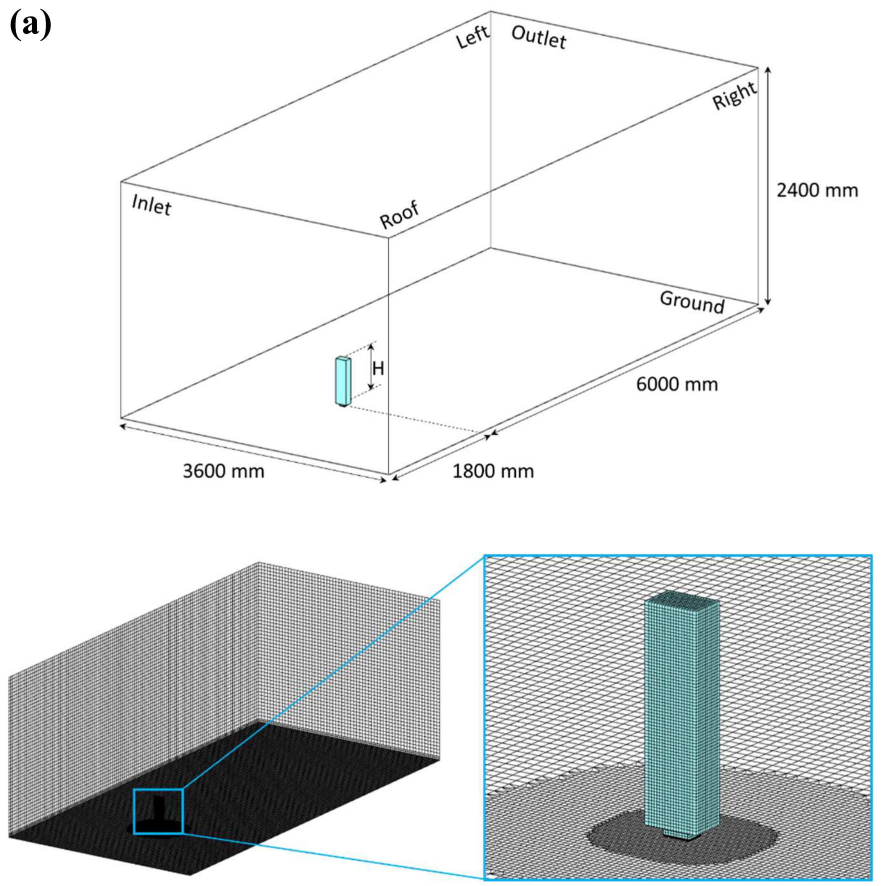

Figure 8. (a) The dimensions of the computational domain, and (b) the grid arrangement in the computation domain and around the lift-up building.

The CFD simulations were conducted as steady 3-D RANS simulations using the realizable *k*-*ε* turbulence model. The inlet boundary conditions were provided as the profiles of mean wind speed (*U*), turbulent kinetic energy (*k*), and turbulent kinetic energy dissipation rate (*ε*) (Figure 9), as derived with Eqs. (3) – (5) using data from the wind tunnel tests conducted by Tse et al. [16] and Zhang et al. ([17], [18]). The ground was modelled as a rough wall with the sand-equivalent roughness height K_s = 0.00027 m and roughness coefficient Cs = 0.5, while building walls were modelled as smooth walls. The standard wall function by Launder and Spalding [53] was used at the walls. The symmetry boundary condition, where $\frac{\partial}{\partial y} \, and \, \frac{\partial}{\partial z}(u, v, w, k, \varepsilon) = 0$

was assigned to the lateral and top boundaries of the computational domain and the outflow boundary condition ($\frac{\partial}{\partial x}\,and\,\frac{\partial}{\partial y}(u,v,w,k,\varepsilon)=0$) was applied to the outlet.

$$U(z)=U_{ref}\left(\frac{z}{z_{ref}}\right)^{\alpha} \tag{3}$$

where U_{ref} is the reference wind speed 7.5 ms^{-1} at the reference height, z_{ref} = 0.6 m and α is the power-law exponent equal to 0.12.

$$k(z)=\left(I(z)U(z)\right)^{2} \tag{4}$$

where *I(z)* is the vertical profile of turbulence intensity measured in the wind tunnel test.

$$\varepsilon(z)=C_{\mu}^{1/2}k(z)\frac{U_{ref}}{z_{ref}}\alpha\left(\frac{z}{z_{ref}}\right)^{(\alpha-1)} \tag{5}$$

where C_{μ} is a constant with a value of 0.09

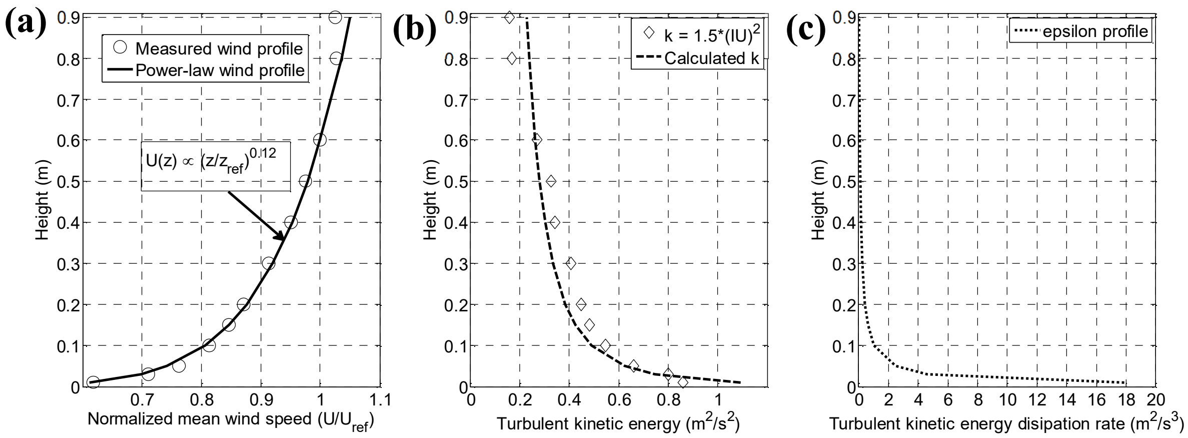

Figure 12. Inflow boundary conditions of CFD simulations (a) mean wind speed profile (*U*), (b) turbulent kinetic energy (*k*) profile, (c) turbulent kinetic energy dissipation (ε) profile.

The SIMPLE algorithm was employed for pressure-velocity coupling and pressure interpolation was second order. All the convective and viscous terms were solved using the second-order discretisation scheme. The convergence of the CFD results was assumed when the residual of x-, y-, z-momentum, k, ε, and continuity reached to 10^{-5}. After the CFD simulations were converged, the wind speed at the pedestrian level was extracted and processed to calculate P_{com} and T_{com} values. The entire CFD simulation procedure was automated using a MATLAB code that generated building geometry, constructed the computational domain, created the computational grid, applied boundary conditions and solver settings, run the simulation and extracted mean wind speed at the pedestrian level.

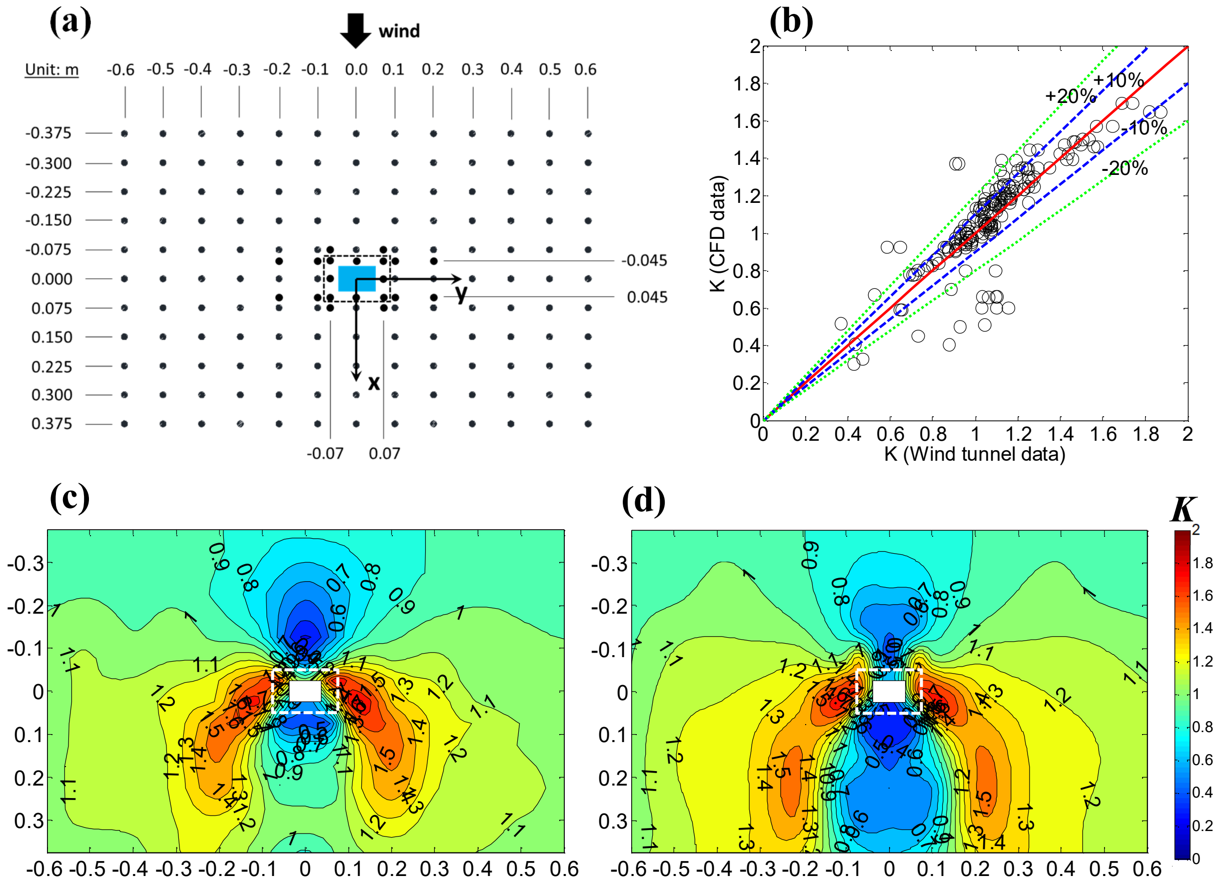

Figure 13. (a) Measurement locations around the lift-up building, (b) comparison of K values in CFD simulation and the wind tunnel test, and the distribution of K value near the lift-up building in (c) the wind tunnel test, (d) the CFD simulation.

Accuracy of CFD simulations in this study was estimated by comparing the mean wind speed extracted from a CFD simulation with data from a wind tunnel test conducted by Tse et al. [16]. The mean wind speed at the pedestrian level near a lift-up building (H=120 m, W= 30 m, D=20 m, h=6 m, w=15 m, d=10 m in full scale) was measured at 169 points as shown in Figure 10(a). The measurement points covered an area of 240 m × 150 m similar to the interrogated area used in the optimization procedure. Figure 10(b) shows the comparison of K value calculated using the wind speed data from the CFD simulation and the wind tunnel tests. The two sets of data agree well with each other in high wind speed areas (K > 1.2) while the data from CFD simulation have larger discrepancies (larger than 20%) with respect to those of the wind tunnel test in the areas with low wind speeds (K<1). Such discrepancies may be attributed to a well-known shortcoming of RANS simulation in under-predicting low wind speeds near buildings. Nevertheless, CFD simulation still capture important flow features near buildings (Figure 10 (d)) as accurately as the wind tunnel (Figure 10(c))

3. RESULTS AND DISCUSSION

The optimization process was conducted as two single-objective optimizations: to maximize the areas with pedestrian (1) wind comfort and (2) thermal comfort; and as a multi-objective optimization to simultaneously maximize the area with pedestrian wind and thermal comfort near lift-up buildings in 'hot-calm 'and 'cold-windy 'climates. The results of these optimizations in terms of the evolution of the lift-up design, the best lift-up design for the selected objective function(s), the corresponding building dimensions and orientation, and the areas with pedestrian wind and thermal comfort are, separately, as follows:

3.1.Optimization of the lift-up design for pedestrian wind comfort.

Optimization was conducted over 200 generations to obtain the optimum lift-up design to generate the largest area with pedestrian wind comfort near the lift-up building. Figure 14 shows how the area with pedestrian comfort (P_{com}) grows over generations in four separate optimization runs. Here the optimization was run four times to ensure that the framework methodically selected the best lift-up design rather than something arbitrary. For instance, despite different initial P_{com} values: 54.2%, 48.6%, 57.8%, and 59.5% in the four runs, P_{com}

reached its maximum value of 91.8% in the 'hot-calm 'climate in each run (Figure 14(a)). The optimization in cold-wind climate showed a similar trend of increased P_{com}, but the maximum P_{com} value of 55.4% was smaller than that in' hot-calm 'climate (Figure 14(b)). In addition, the optimization process proposed noticeably different lift-up designs in the two climates, as shown in Figures 15 and 16.

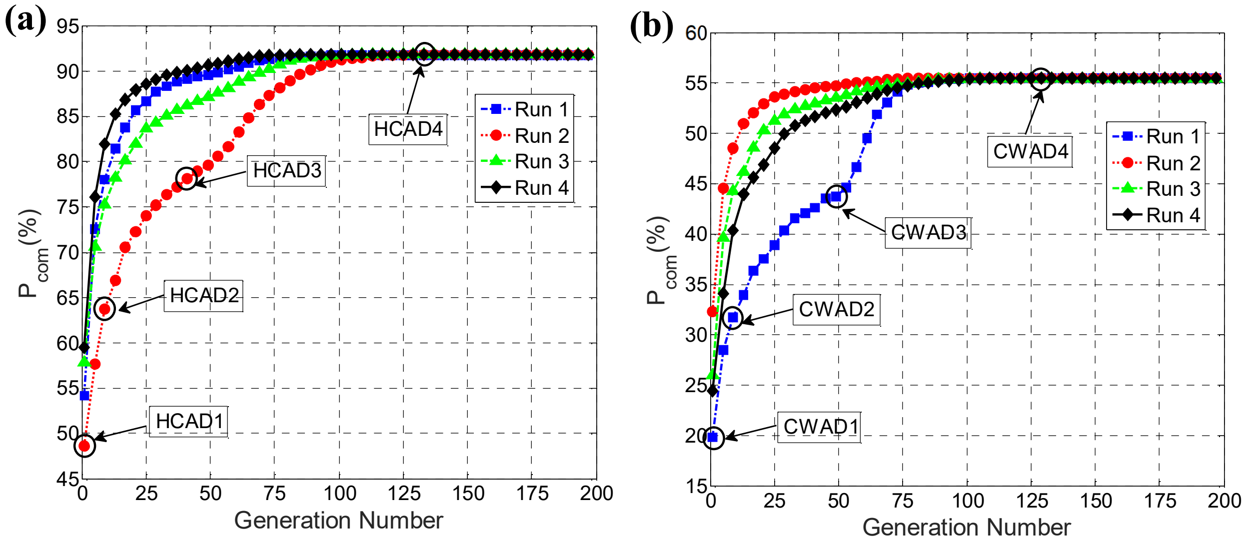

Figure 14. The growth of the area with pedestrian wind comfort (P_{com}) over generations in (a) 'hot-calm' and (b) 'cold-windy' climates.

Figures 15 and 16 show four optimized lift-up designs per each of the two climates, and Figure 17 shows the percentage area of wind speed classes near these buildings calculated according to the relevant wind comfort criteria. From Figures 15 and 17(a), it can be identified that tall intermediate lift-up buildings (1.25>H/W>0.33) such as HCAD1 are not suitable for the 'hot-calm' climate as these buildings create large areas with low wind speeds, while short, intermediate buildings such as HCAD4 emerge as an advantageous lift-up design as it creates large areas with acceptable wind speeds. In fact, the percentage area with comfortable wind speed more than doubled from 42.48% to 88.48% as the lift-up design transformed from HCAD1 to HCAD4. Moreover, the importance of the center core design and building orientation can be identified from comparing a near-optimum design, HCAD3, and optimum design, HCAD4, where the two buildings have comparable dimensions but significantly different center cores and orientations. Zhang et al. ([17], [18]) have tested different center core designs and have concluded that a wide center core creates large areas of low wind speeds in the lift-up area. Those areas can be effectively alleviated by adopting recessed corners to the center core. The effectiveness of recessed corners in creating acceptable wind conditions near lift-up buildings can be identified from Figure 18(b), which shows a smaller area with low wind speed downstream of HCAD4 and a larger area with acceptable wind speed in the lift-up area compared to those of HCAD3 (Figure 18(a)). In addition, the orientation of HCAD4, 27° clockwise from the incident wind direction, influences generating smaller areas with low and high wind speeds upstream and lateral sides of the building, respectively.

In contrast, wide lift-up cores at 0o orientation enhance pedestrian wind comfort near lift-up buildings in 'cold-windy' climate (Figures 16 and 17(b)). In 'cold-windy' climates, lift-up buildings should not only adopt wide center cores but should also have a wide elevated structure such as CWAD4. It is well-known that wide buildings create large areas with wind speed retardation downstream of the buildings ([17], [54], [55]), which in turn provide much necessary wind shelter for pedestrians in windy environments. As can be seen from Figure 19(b), with a wider elevated structure and a center core, CWAD4 creates a large area of acceptable wind speed downstream of the building, while the narrow center core of CWAD3 generates high-speed wind flows in the lift-up area and its narrow elevated structure creates a smaller area with acceptable wind speeds downstream of the building (Figure 19(a)).

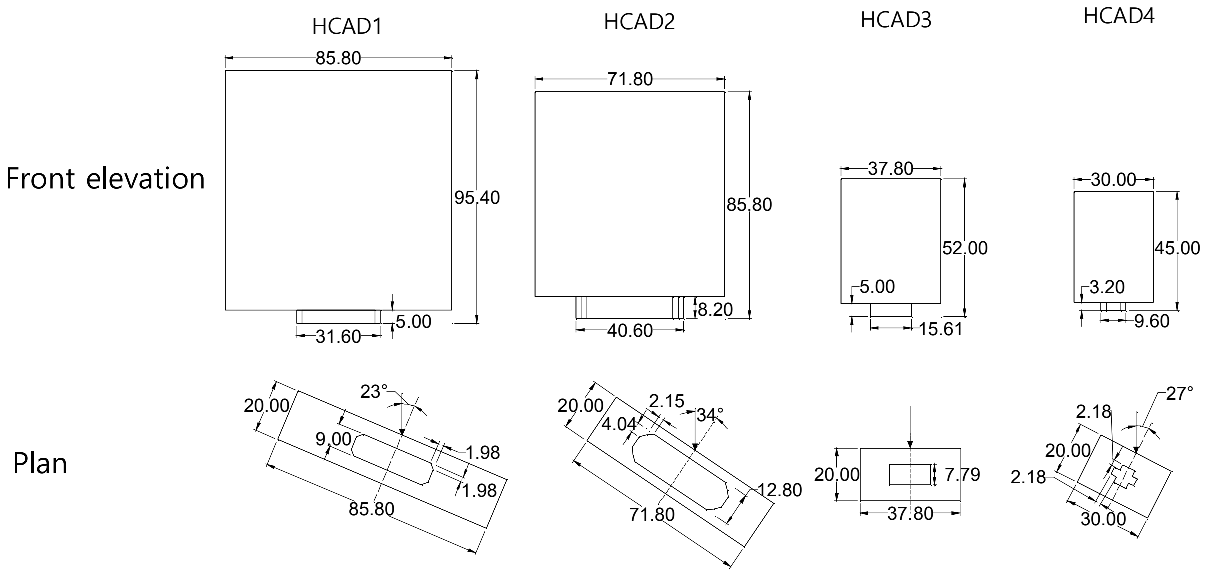

Figure 15. Four selected designs optimized for pedestrian wind comfort in 'hot-calm' climate (dimensions in meters).

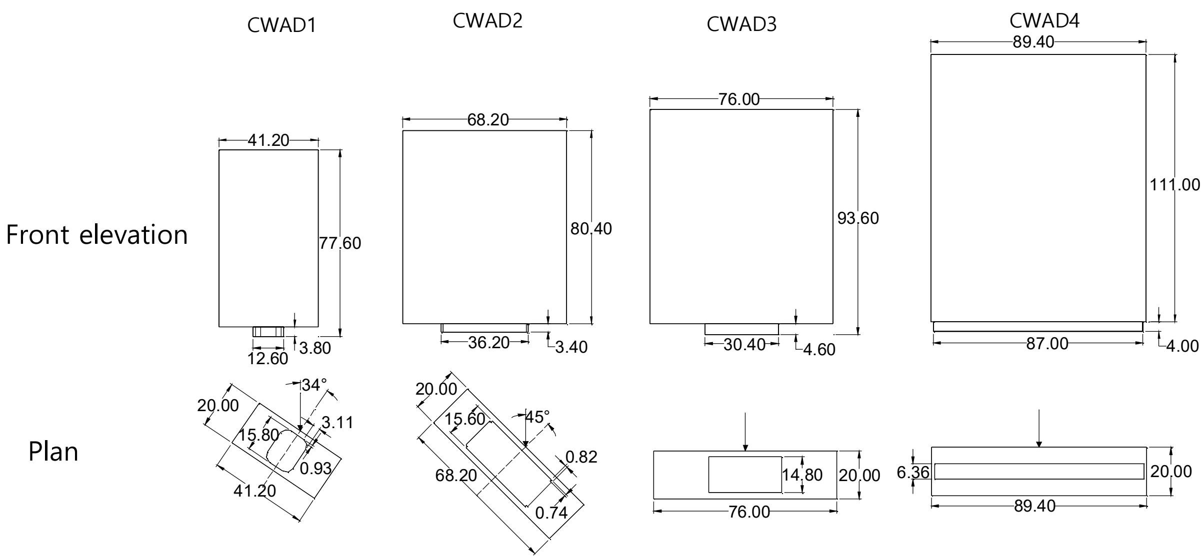

Figure 16. Four designs optimized for pedestrian wind comfort in 'cold-windy' climate (dimensions in meters).

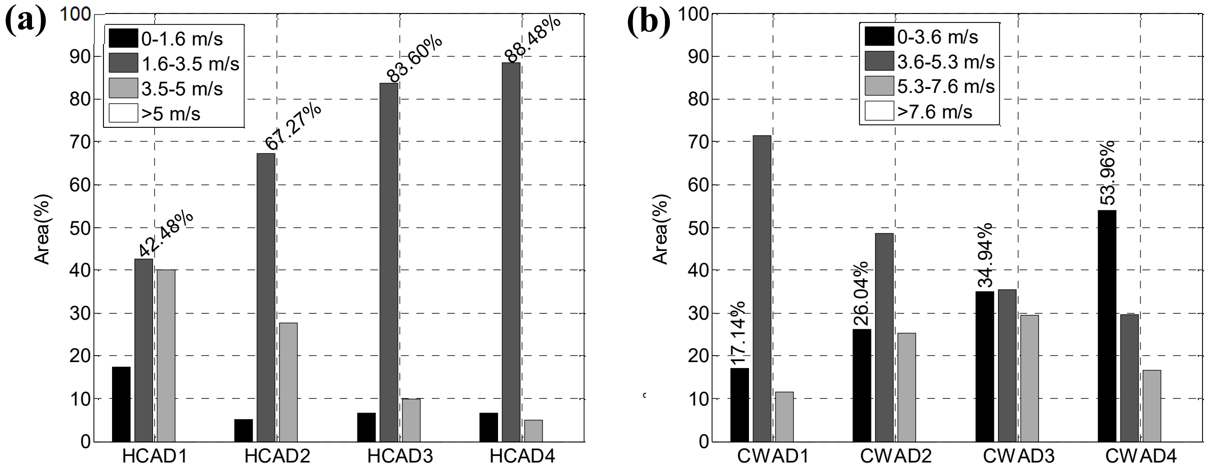

Figure 17. Percentage area of wind speed classes near the selected lift-up buildings in (a) 'hot-calm', and (b) 'cold-windy' climates.

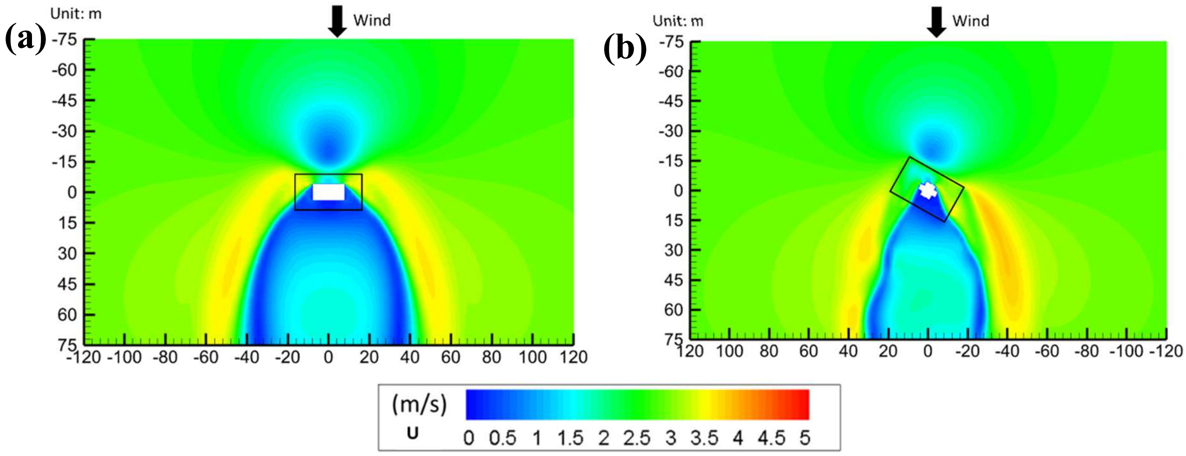

Figure 18. Distribution of pedestrian-level wind speed near (a) a near-optimum lift-up building (HCAD3) and (b) the optimum lift-up building (HCAD4)

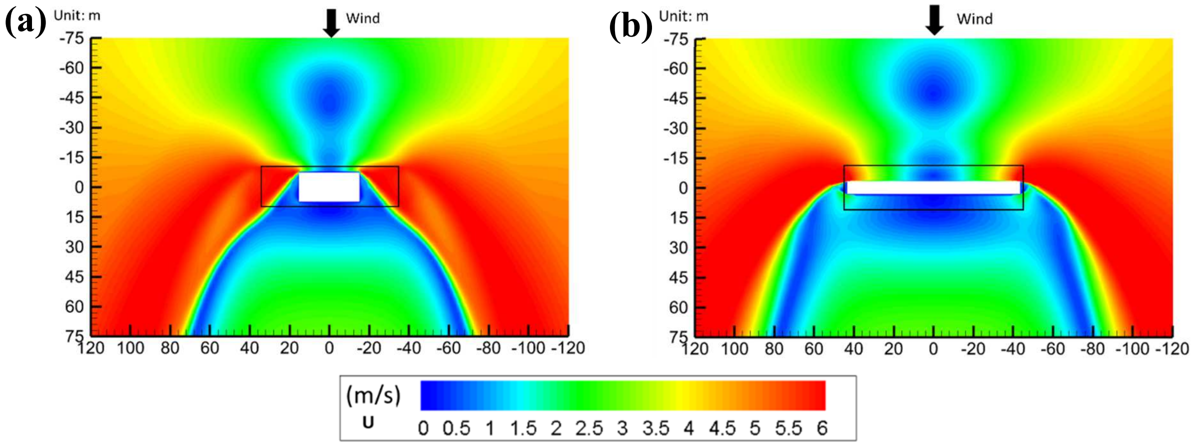

Figure 19. Distribution of pedestrian-level wind speed near (a) a near-optimum lift-up building (CWAD3) and (b) the optimum lift-up building (CWAD4).

3.2. Optimization of the lift-up design for pedestrian thermal comfort.

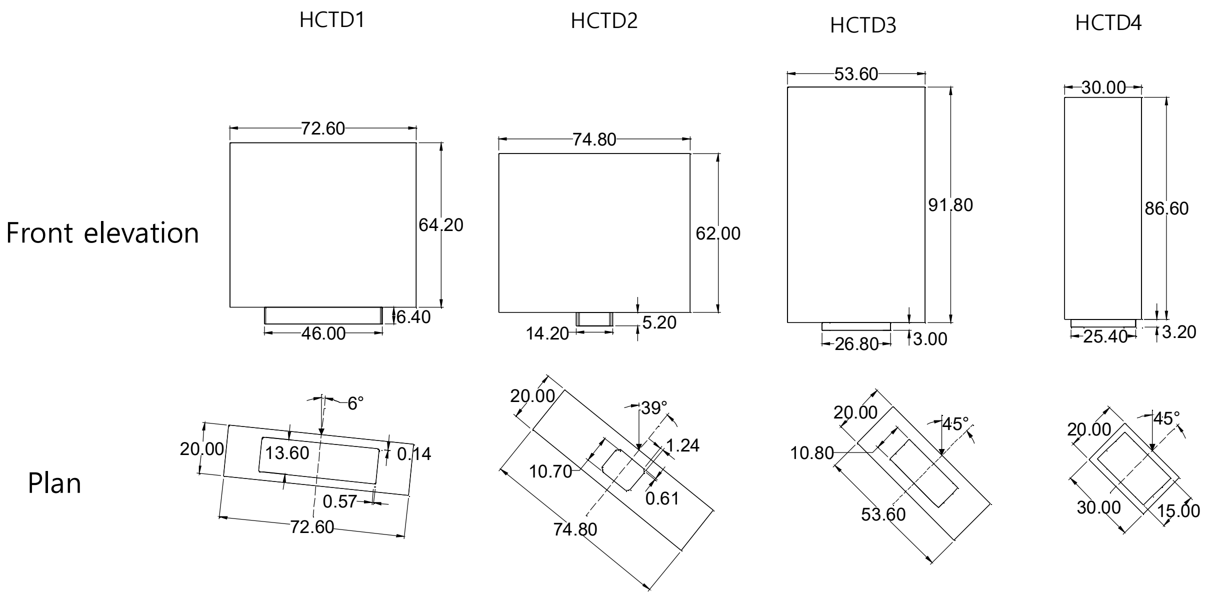

Figure 20. Four designs optimized for pedestrian thermal comfort in 'hot-calm' climate (dimensions in meters).

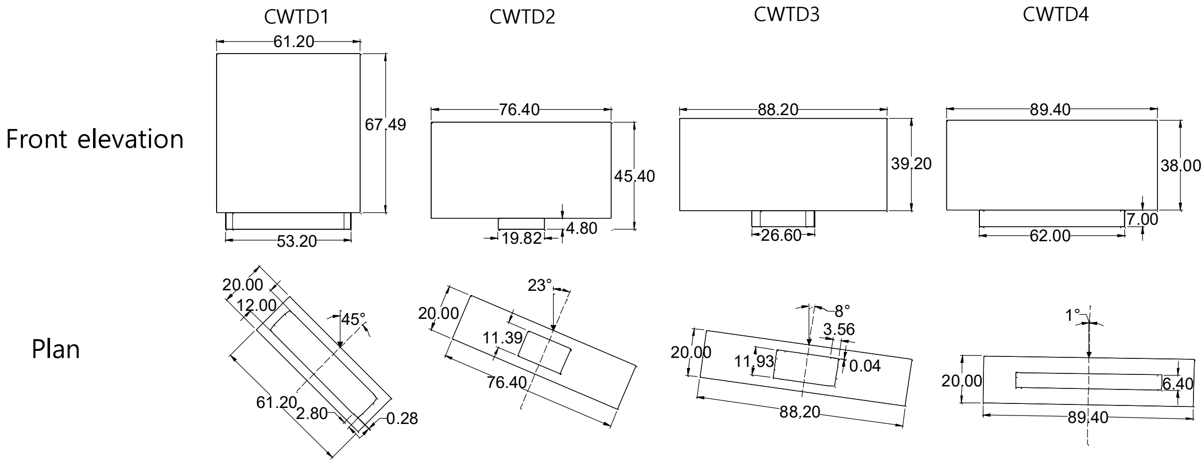

Figure 21. Four designs optimized for pedestrian thermal comfort in 'cold-windy' climate (dimensions in meters)..

Figures 20 and 21 show four lift-up designs including the optimum design for the maximum pedestrian thermal comfort in the two climates obtained from one of the four runs of the optimization process. In contrast to the optimum design HCAD4 to maximize wind comfort, the lift-up design has evolved into a slender building (H/W>1.25), HCTD4, as the optimum design to maximize the pedestrian thermal comfort in the 'hot-calm' climate. The evolution of the lift-up building causes an increase of T_{com} from 77.98% near HCTD1 to 96.04% near HCTD4 (Figure 22(a)). Although two intermediate lift-up designs; HCTD2 and HCTD3 have comparable T_{com} values to that of the optimum design HCTD4, there is an obvious decreasing trend in area with strong heat stress (UTCI – [32-38 °C]) as the lift-up design evolved from HCTD1 to HCTD4. The reduction of area with strong heat stress near HCTD4 is likely attributed to smaller areas with low wind speeds at the pedestrian level compared with other near optimum designs (Figure 23).

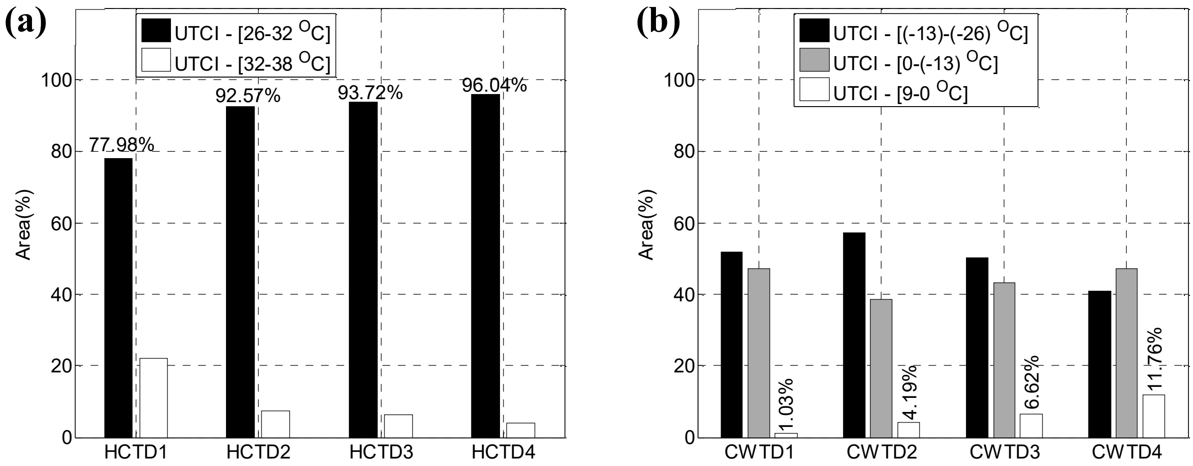

Figure 22. Percentage area of UTCI classes near the selected lift-up buildings in (a) 'hot-calm', and (b) 'cold-windy' climates.

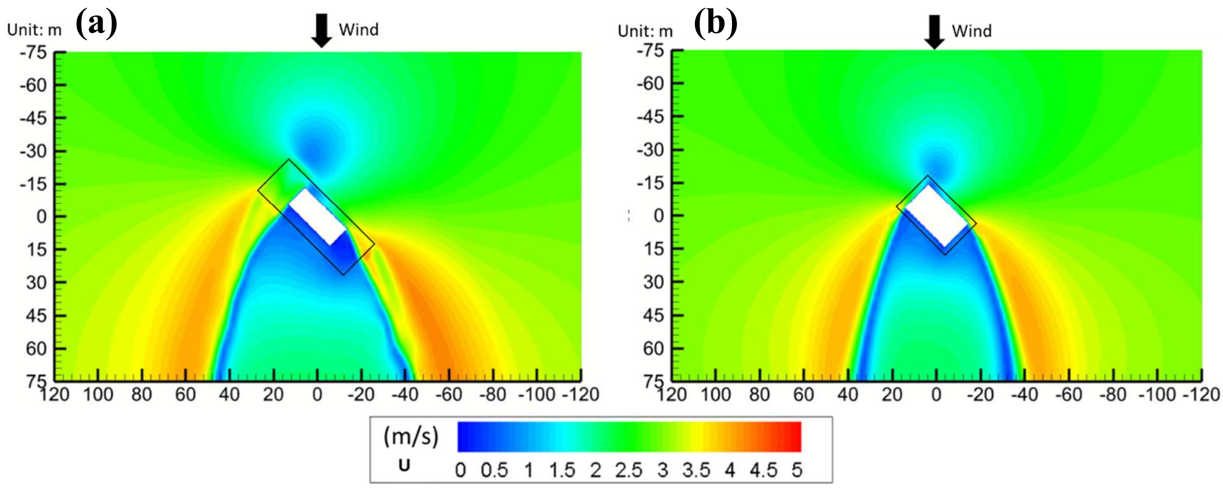

Figure 23. Distribution of pedestrian-level wind speed near (a) a near-optimum lift-up building (HCTD3) and (b) the optimum lift-up building (HCTD4)

Figure 21 illustrates the importance of adopting a wide elevated structure and center core to create pedestrian thermal comfort in 'cold-windy' climates where three out of four designs (CWTD2, CWTD3, and CWTD4) have either one or both aforementioned features. With a wide elevated structure and a center core, the optimum lift-up design CWTD4 has a larger area with slight cold stress (UTCI – [+9-0 °C]) of 11.76% (Figure 22(b)) than CWTD1 (1.03%), which only has a wide center core. It is noteworthy that CWTD4 does not only generate a large area with slight cold stress but also simultaneously decreases the size of the area with strong cold stress (UTCI – [(-13)-(-27) °C]) (area = 41.05%) compared to that found near other three lift-up designs (CWTD1-51.8%; CWTD2-57.19%; CWTD3-50.25%). As can be seen from Figure 24, two factors — a large area with low wind speed and a smaller area with high wind speed in the separation layers — may cause the reduction of area with strong cold stress near CWTD4, as compared with the near-optimum solution CWTD3.

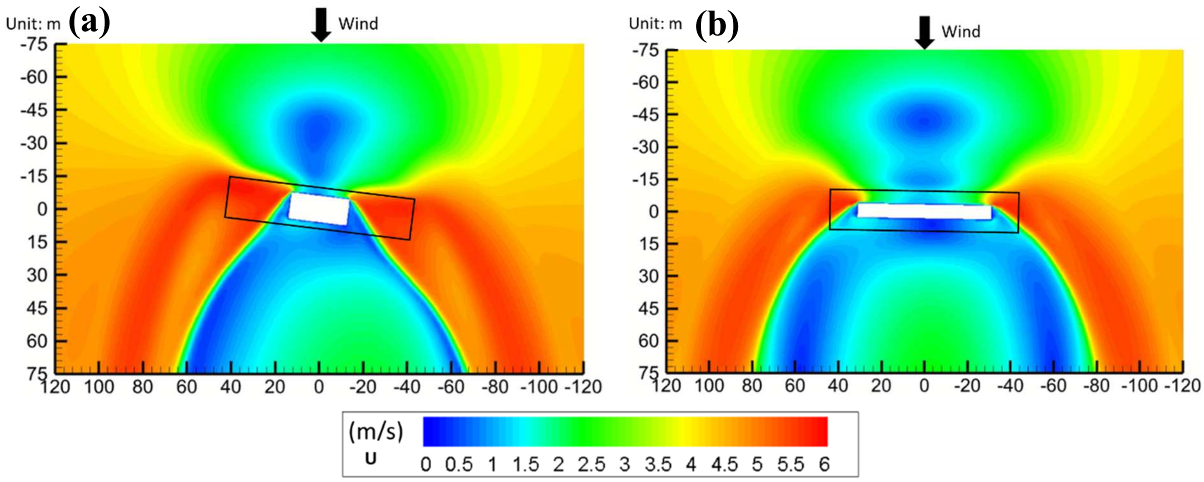

Figure 24. Distribution of pedestrian-level wind speed near (a) a near-optimum lift-up building (CWTD3) and (b) the optimum lift-up building (CWTD4).

3.3. Multi-objective optimization

Sections 3.1 and 3.2 show that if each optimization uses only one objective function — e.g., *either* to maximize wind comfort *or* thermal comfort — their optimum designs can diverge substantially. For 'hot-calm' climate, for example, the optimum design for wind comfort was an intermediate building with small center core; for thermal comfort it was a slender building with wide center. This discrepancy is attributed to the differential contribution of wind to pedestrian wind and thermal comfort: high wind, for example, enhances thermal comfort in 'hot-calm' climate, but may cause wind discomfort for pedestrians. This makes it difficult to select the best 'lift-up' design if the requirement is to maximize area with pedestrian wind and thermal comfort simultaneously. With two objective functions, the optimization process becomes a multi-objective optimization and it can have more than one optimum lift-up design, which creates different sizes of area with pedestrian wind and thermal comfort in the surrounding. The set of optimal solutions in a multi-objective optimization is known as the Pareto frontier and two Pareto frontiers found from the multi-objective optimization of the lift-up design in 'hot-calm' and 'cold-wind' climates are shown in Figure 25.

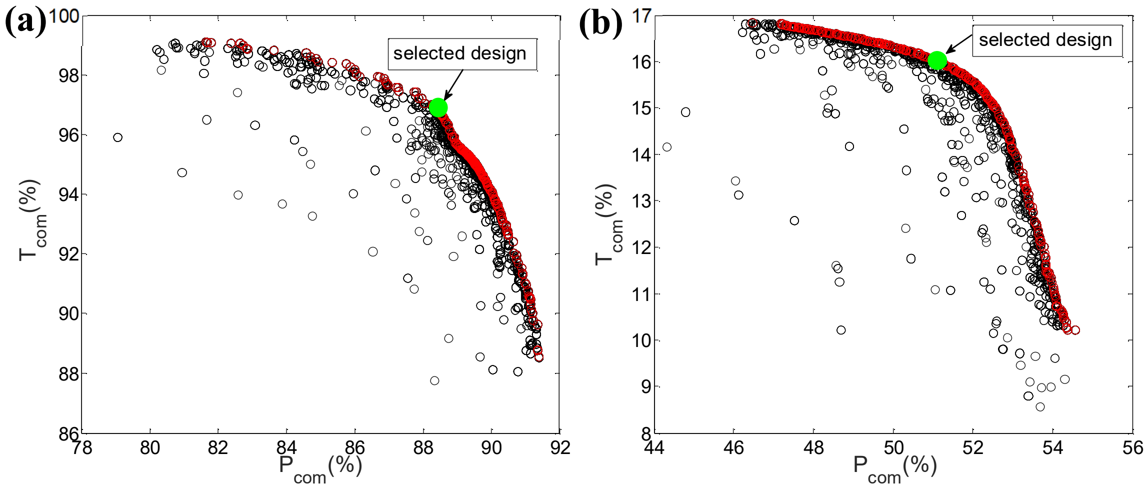

Figure 25. The Pareto frontier of lift-up design in (a) 'hot-calm' and (b) 'cold-windy' climates.

The Pareto frontiers shown in Figure 25 were constructed using non-dominated sorting genetic algorithm II (NSGA II) and a crowd-distance calculation [56]. Since every data point on the Pareto frontier represents an optimal 'lift-up 'design, it is necessary to select one design as the final design. The selection can be made using a decision-making technique such as the linear programming technique for multidimensional analysis of preference (LINMAP) [57], the technique for order preference by similarity to ideal solution (TOPSIS) [58], or Shannon's entropy method [59]. In this study, two optimal lift-up designs, as shown in Figure 26, were selected from the Pareto frontiers using the LINMAP technique. LINMAP first calculates the Euclidean distance of each point on the Pareto frontier from the ideal point (D_{i+}), which optimizes each objective function without taking account of other objective functions and then select the point on Pareto frontier with minimum distance from the ideal solution (i.e., $i_{final} = i \in \min(D_{i+})$). The value D_{i+} is calculated as in Eq. (6).

$$D_{i+} = \sqrt{\sum_{j=1}^{n} \left(F_{ij} - F_j^{ideal}\right)^2} \tag{6}$$

In Eq. (6), n is the number of objective functions, i is each route on the Pareto frontier i.e., i=1, 2, 3, ..., m, F_j^{ideal} is the ideal value for the j^{th} objective function obtained by a single objective optimization.

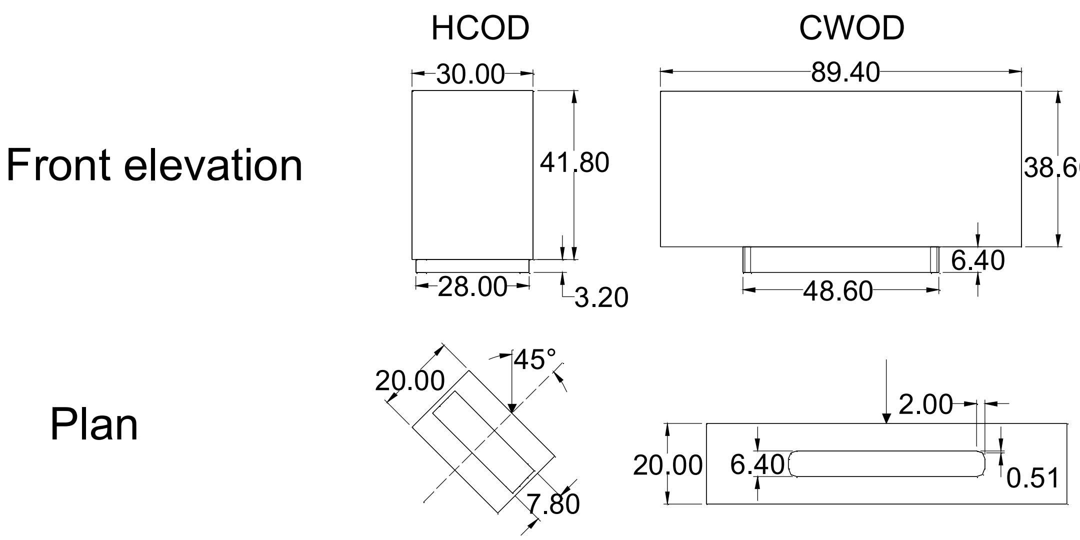

Figure 26. Two selected lift-up designs from the multi-objective optimization process in the 'hot-calm' (HCOD) and 'cold-windy'(CWOD) climates (dimensions in meters).

The dimensions of the two selected lift-up designs for 'hot-calmand' and 'cold-wind' climates are shown in Figure 26. The optimal lift-up designs have P_{com} and T_{com} values 90.80% and 97.46% of HCOD and 44.32% and 8.97% of CWOD and they are different from those of the single-objective optimization. Moreover, though not completely similar, the optimal designs in multi-objective and single-objective optimization still show some similarities: for instance, the multi-objective optimization in 'hot-calm' climate selects a short, intermediate elevated structure (Figure 26) similar to the optimum lift-up design to maximize pedestrian wind comfort in these conditions (Figure 15) but it has a wide center core, which is similar to that found for the single objective optimization of pedestrian thermal conditions (Figure 16). In addition, the 45° orientation of HCOD is advantageous in creating a narrow area with low wind speeds and fairly intense separation layers to achieve both pedestrian wind and thermal comfort (Figure 27(a)). Conversely, the lift-up design for 'cold-windy' climate shown in Figure 26 and the distribution of wind speed at the pedestrian level (Figure 27(b)) closely resemble those of the optimum design found for pedestrian thermal comfort in these conditions. Therefore, it is prudent to assume that pedestrian thermal comfort may be the governing factor in designing lift-up buildings in 'cold-windy' climate.

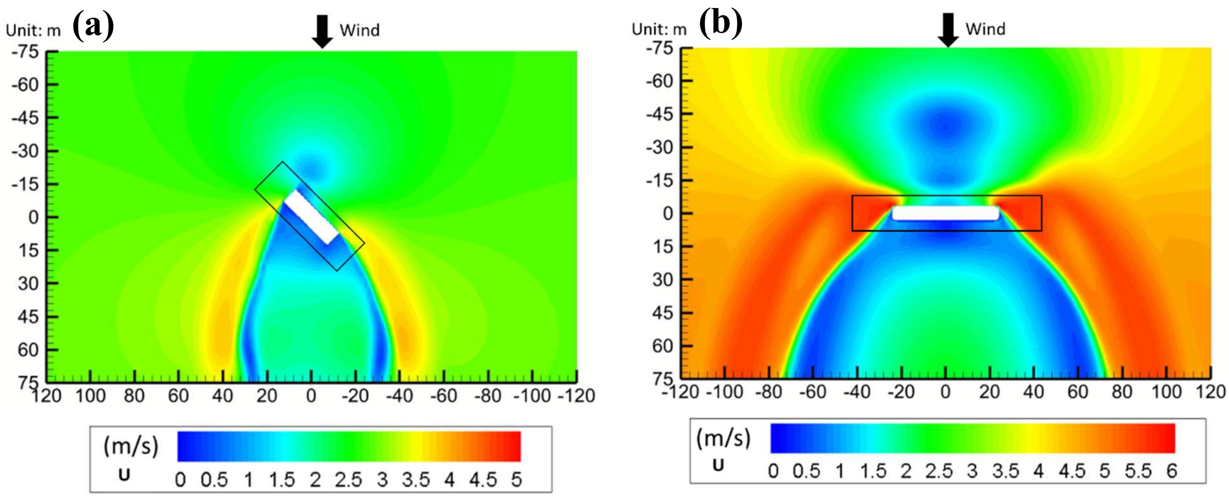

Figure 27. Distribution of pedestrian-level wind speed near the optimum lift-up designs obtained from multi-objective optimization for (a) 'hot-calm' (HCOD) and (b) 'cold-windy' (CWOD) climates

4. LIMITATIONS OF THE STUDY

Although the proposed framework shows promise in achieving and maintaining acceptable wind and thermal environments near lift-up buildings, it has some inherent shortcomings:

1. 3-D SRANS CFD simulation has been used to develop the ANN-based surrogate model: the two-equation turbulence closure model such as the realizable k-ε model used in this study has been known to under-predict low wind speeds near buildings ([60], [61]). This

shortcoming would lead to the wind and thermal comfort in the 'hot-calm' and 'cold-windy' climates getting under- and over-predicted respectively. It is prudent to use better turbulence modeling such as large eddy simulation (LES) for developing the surrogate model and evaluating the PLWE, but the required computation power would be excessive for this type of studies.

2. The GA and LINMAP were used in this study to optimize the 'lift-up' design and select an optimal design from the Pareto frontier; they are only two among various evolutional optimization algorithms and decision-making techniques. These other techniques should also be considered and compared.
3. This study followed the unconstrained optimization, in which all eight design parameters can be modified within their upper and lower bounds to obtain the optimum lift-up design. In reality, some or all of these design parameters are restricted at certain values (e.g. H=100 m), leading to the constrained optimization of the lift-up design. Consequently, P_{com} and T_{com} can be substantially different between constrained and unconstrained optimization. Constrained optimization can also indicate which are the governing design parameters by analyzing how they influence P_{com} and T_{com}.

5. CONCLUDING REMARKS

This study has proposed a framework that combines CFD simulation, ANN-based surrogate model, and optimization algorithm to modify the lift-up design to maximize pedestrian wind and thermal comfort near lift-up buildings in 'hot-calm' and 'cold-windy' climates. The framework can propose the most suitable values for eight parameters for a 'lift-up' design based on the requirement of maximizing the area with pedestrian wind comfort or thermal comfort or both in the two climates. The proposed framework can improve the lift-up design to increase the area with pedestrian wind comfort by more than 46% and 37% and the area with pedestrian thermal comfort by 18% and 10% near the lift-up buildings in 'hot-calm' and 'cold-windy' climates, respectively. Furthermore, the optimal lift-up designs found for different objective functions suggest that a short, intermediate elevated building with a smaller center core with recessed corners is advantageous for creating pedestrian wind comfort near lift-up buildings in 'hot-calm' climates and in these conditions wide, tall intermediate lift-up buildings with a wide center core are necessary to maintain acceptable outdoor thermal environment for pedestrians. Slender elevated buildings with wide center cores are suitable for maintaining acceptable pedestrian-level wind conditions in 'cold-windy' climates, but the elevated building should be short and wide to alleviate pedestrians from strong cold stress. Indeed, pedestrian thermal comfort could be the governing factor in designing lift-up buildings in 'cold-windy' climates.

ACKNOWLEDGEMENT

The work described in this paper was partially supported by the grants from the Research Grants Council (RGC) of the HKSAR, China by the General Research Fund (GRF) 17250616 and the Collaborative Research Fund (CRF) HKU C7064-18G.

REFERENCES

[1]. "*Land Utilization in Hong Kong 2018*", Planning Department, the Government of the Hong Kong Special Administrative Region, Accessed on: Nov. 11, 2019. [Online]. Available: https://www.pland.gov.hk/pland_en/info_serv/statistic/landu.html

[2]. E. Ng, "Policies and technical guidelines for urban planning of high-density cities – air ventilation assessment (AVA) of Hong Kong," *Building and Environment*, vol. 44, no. 7, pp. 1478–1488, 2009.

[3]. E. Ng, C. Yuan, L. Chen, C. Ren, and J. C. Fung, "Improving the wind environment in high-density cities by understanding urban morphology and surface roughness: A study in Hong Kong," *Landscape and Urban Planning*, vol. 101, no. 1, pp. 59–74, 2011.

[4]. C. Yuan and E. Ng, "Building porosity for better urban ventilation in high-density cities – A computational parametric study," *Building and Environment*, vol. 50, pp. 176–189, 2012.

[5]. V. Cheng, E. Ng, C. Chan, and B. Givoni, "Outdoor thermal comfort study in a sub-tropical climate: a longitudinal study based in Hong Kong," *International Journal of Biometeorology*, vol. 56, no. 1, pp. 43–56, Jan. 2011.

[6]. T. Wang, "A study of surface ozone and the relation to complex wind flow in Hong Kong," *Atmospheric Environment*, vol. 35, no. 18, pp. 3203–3215, 2001.

[7]. M. S. Wong, J. E. Nichol, P. H. To, and J. Wang, "A simple method for designation of urban ventilation corridors and its application to urban heat island analysis," *Building and Environment*, vol. 45, no. 8, pp. 1880–1889, 2010.

[8]. C. Yip, W. L. Chang, K. H., Yeung and I. T Yu, "Possible meteorological influence on the severe acute respiratory syndrome (SARS) community outbreak at Amoy Gardens, Hong Kong," *Journal of environmental health*, 70(3), pp. 39-47, 2007.

[9]. O. Coceal, T. G. Thomas, I. P. Castro, and S. E. Belcher, “Mean Flow and Turbulence Statistics Over Groups of Urban-like Cubical Obstacles,” *Boundary-Layer Meteorology*, vol. 121, no. 3, pp. 491–519, Mar. 2006.

[10]. T. Kubota, M. Miura, Y. Tominaga, and A. Mochida, “Wind tunnel tests on the relationship between building density and pedestrian-level wind velocity: Development of guidelines for realizing acceptable wind environment in residential neighborhoods,” *Building and Environment*, vol. 43, no. 10, pp. 1699–1708, 2008.

[11]. S. Yim, J. Fung, A. Lau, and S. Kot, “Air ventilation impacts of the ‘wall effect’ resulting from the alignment of high-rise buildings,” *Atmospheric Environment*, vol. 43, no. 32, pp. 4982–4994, 2009.

[12]. J. Hang, M. Sandberg, Y. Li, and L. Claesson, “Pollutant dispersion in idealized city models with different urban morphologies,” *Atmospheric Environment*, vol. 43, no. 38, pp. 6011–6025, 2009.

[13]. T. Hu and R. Yoshie, “Indices to evaluate ventilation efficiency in newly-built urban area at pedestrian level,” *Journal of Wind Engineering and Industrial Aerodynamics*, vol. 112, pp. 39–51, 2013.

[14]. “*Sustainable Building Design Guidelines*” Building Department, the Government of the Hong Kong Special Administrative Region, Accessed on: Nov. 11, 2019. [Online]. Available: https://www.bd.gov.hk/doc/en/resources/codes-and-references/practice-notes-and-circular-letters/pnap/APP/APP152.pdf

[15]. Q. Xia, X. Liu, J. Niu, and K. C. S. Kwok, “Effects of building lift-up design on the wind environment for pedestrians,” *Indoor and Built Environment*, vol. 26, no. 9, pp. 1214–1231, 2015.

[16]. K. Tse, X. Zhang, A. Weerasuriya, S. Li, K. Kwok, C. M. Mak, and J. Niu, "Adopting 'lift-up' building design to improve the surrounding pedestrian-level wind environment," *Building and Environment*, vol. 117, pp. 154–165, 2017.

[17]. X. Zhang, K. Tse, A. Weerasuriya, S. Li, K. Kwok, C. M. Mak, J. Niu, and Z. Lin, "Evaluation of pedestrian wind comfort near 'lift-up' buildings with different aspect ratios and central core modifications," *Building and Environment*, vol. 124, pp. 245–257, 2017.

[18]. X. Zhang, K. Tse, A. Weerasuriya, K. Kwok, J. Niu, Z. Lin, and C. M. Mak, "Pedestrian-level wind conditions in the space underneath lift-up buildings," *Journal of Wind Engineering and Industrial Aerodynamics*, vol. 179, pp. 58–69, 2018.

[19]. Y. Du, C. M. Mak, J. Liu, Q. Xia, J. Niu, and K. Kwok, "Effects of lift-up design on pedestrian level wind comfort in different building configurations under three wind directions," *Building and Environment*, vol. 117, pp. 84–99, 2017.

[20]. Y. Du, C. M. Mak, K. Kwok, K.-T. Tse, T.-C. Lee, Z. Ai, J. Liu, and J. Niu, "New criteria for assessing low wind environment at pedestrian level in Hong Kong," *Building and Environment*, vol. 123, pp. 23–36, 2017.

[21]. Y. Du, C. M. Mak, T. Huang, and J. Niu, "Towards an integrated method to assess effects of lift-up design on outdoor thermal comfort in Hong Kong," *Building and Environment*, vol. 125, pp. 261–272, 2017.

[22]. J. Liu, J. Niu, C. M. Mak, and Q. Xia, "Detached eddy simulation of pedestrian-level wind and gust around an elevated building," *Building and Environment*, vol. 125, pp. 168–179, 2017.

[23]. J. Liu, X. Zhang, J. Niu, and K. T. Tse, "Pedestrian-level wind and gust around buildings with a 'lift-up' design: Assessment of influence from surrounding buildings by adopting LES," *Building Simulation*, vol. 12, no. 6, pp. 1107–1118, 2019.

[24]. Y. Du, C. M. Mak, and Y. Li, “Application of a multi-variable optimization method to determine lift-up design for optimum wind comfort,” *Building and Environment*, vol. 131, pp. 242–254, 2018.

[25]. W.J. Beranek, “Wind environment around single buildings of rectangular shape,” *Heron*, 29 (1), pp. 4–31, 1984.

[26]. J. Gandemer, "Wind environment around buildings: aerodynamic concepts." In Proc., 4th Int. Conf. Wind Effects on Buildings and Structures, Heathrow, pp. 423-432. 1975.

[27]. W.H. Melbourne, P.J. Joubert, “Problems of wind flow at the base of tall buildings,” In: Proceedings Wind Effects on Buildings and Structures, Tokyo. 1971.

[28]. A. D. Penwarden and A. F. E. Wise, *Wind environment around buildings*. London: Her Majestys Stationery Office, 1975.

[29]. T. Stathopoulos, H. Wu, and C. Bédard, “Wind environment around buildings: A knowledge-based approach,” *Journal of Wind Engineering and Industrial Aerodynamics*, vol. 44, no. 1-3, pp. 2377–2388, 1992.

[30]. J. M. Gimenez and F. Bre, “Optimization of RANS turbulence models using genetic algorithms to improve the prediction of wind pressure coefficients on low-rise buildings,” *Journal of Wind Engineering and Industrial Aerodynamics*, vol. 193, p. 103978, 2019.

[31]. A. Elshaer, G. Bitsuamlak, and A. E. Damatty, “Enhancing wind performance of tall buildings using corner aerodynamic optimization,” *Engineering Structures*, vol. 136, pp. 133–148, 2017.

[32]. A. Elshaer and G. Bitsuamlak, “Multiobjective Aerodynamic Optimization of Tall Building Openings for Wind-Induced Load Reduction,” *Journal of Structural Engineering*, vol. 144, no. 10, p. 04018198, 2018.

[33]. S. Jung, J. Ghaboussi, and S.-D. Kwon, "Estimation of Aeroelastic Parameters of Bridge Decks Using Neural Networks," *Journal of Engineering Mechanics*, vol. 130, no. 11, pp. 1356–1364, 2004.

[34]. T. Wu and A. Kareem, "Modeling hysteretic nonlinear behavior of bridge aerodynamics via cellular automata nested neural network," *Journal of Wind Engineering and Industrial Aerodynamics*, vol. 99, no. 4, pp. 378–388, 2011.

[35]. Y. Chen, G. Kopp, and D. Surry, "Prediction of pressure coefficients on roofs of low buildings using artificial neural networks," *Journal of Wind Engineering and Industrial Aerodynamics*, vol. 91, no. 3, pp. 423–441, 2003.

[36]. E. English and F. Fricke, "The interference index and its prediction using a neural network analysis of wind-tunnel data," *Journal of Wind Engineering and Industrial Aerodynamics*, vol. 83, no. 1-3, pp. 567–575, 1999.

[37]. A. Khanduri, C. Bédard, and T. Stathopoulos, "Modelling wind-induced interference effects using backpropagation neural networks," *Journal of Wind Engineering and Industrial Aerodynamics*, vol. 72, pp. 71–79, 1997.

[38]. G. T. Bitsuamlak, C. Bédard, and T. Stathopoulos, "Modeling the Effect of Topography on Wind Flow Using a Combined Numerical–Neural Network Approach," *Journal of Computing in Civil Engineering*, vol. 21, no. 6, pp. 384–392, 2007.

[39]. A. U. Weerasuriya, Xuelin Zhang, K. T. Tse, "An ANN-based surrogate model for predicting pedestrian-level wind environment," in the Proc. 8th International Conference on environmental effects on buildings and people: actions, influences, interactions, discomfort (EEBP8), October 3-5, 2018 Cracow, Poland.

[40]. A. U. Weerasuriya, K. T. Tse, Xuelin Zhang, and K. C. S. Kwok, "Integrating twisted wind profiles to Air Ventilation Assessment (AVA): The current status," *Building and Environment*, vol. 135, pp. 297–307, 2018.

[41]. A. Lai, M. Maing, and E. Ng, “Observational studies of mean radiant temperature across different outdoor spaces under shaded conditions in densely built environment,” *Building and Environment*, vol. 114, pp. 397–409, 2017.

[42]. W. Janssen, B. Blocken, and T. V. Hooff, “Pedestrian wind comfort around buildings: Comparison of wind comfort criteria based on whole-flow field data for a complex case study,” *Building and Environment*, vol. 59, pp. 547–562, 2013.

[43]. K. K.-L. Lau, F. Lindberg, D. Rayner, and S. Thorsson, “The effect of urban geometry on mean radiant temperature under future climate change: a study of three European cities,” *International Journal of Biometeorology*, vol. 59, no. 7, pp. 799–814, 2014.

[44]. T. Lawson, “The widn content of the built environment,” *Journal of Wind Engineering and Industrial Aerodynamics*, vol. 3, no. 2-3, pp. 93–105, 1978.

[45]. A. Penwarden, “Acceptable wind speeds in towns,” *Building Science*, vol. 8, no. 3, pp. 259–267, 1973.

[46]. P. O. Fanger, "Thermal comfort. Analysis and applications in environmental engineering." *Thermal comfort. Analysis and applications in environmental engineering*, 1970.

[47]. P. Höppe, “The physiological equivalent temperature - a universal index for the biometeorological assessment of the thermal environment,” *International Journal of Biometeorology*, vol. 43, no. 2, pp. 71–75, 1999.

[48]. A. P. Gagge, A.P. Fobelets, and P.E. Berglund, “A standard predictive index of human response to the thermal environment,” *ASHRAE Transactions*, 92, pp. 709-731, 1986.

[49]. G. Jendritzky, R. D. Dear, and G. Havenith, “UTCI—Why another thermal index?,” *International Journal of Biometeorology*, vol. 56, no. 3, pp. 421–428, 2011.

[50]. Z. Fang, X. Feng, J. Liu, Z. Lin, C. M. Mak, J. Niu, K.-T. Tse, and X. Xu, "Investigation into the differences among several outdoor thermal comfort indices against field survey in subtropics," *Sustainable Cities and Society*, vol. 44, pp. 676–690, 2019.

[51]. P. Bröde, D. Fiala, K. Błażejczyk, I. Holmér, G. Jendritzky, B. Kampmann, B. Tinz, and G. Havenith, "Deriving the operational procedure for the Universal Thermal Climate Index (UTCI)," *International Journal of Biometeorology*, vol. 56, no. 3, pp. 481–494, 2011.

[52]. Y. Tominaga, A. Mochida, R. Yoshie, H. Kataoka, T. Nozu, M. Yoshikawa, and T. Shirasawa, "AIJ guidelines for practical applications of CFD to pedestrian wind environment around buildings," *Journal of Wind Engineering and Industrial Aerodynamics*, vol. 96, no. 10-11, pp. 1749–1761, 2008.

[53]. B. Launder and D. Spalding, "The Numerical Computation of Turbulent Flows," *Numerical Prediction of Flow, Heat Transfer, Turbulence and Combustion*, pp. 96–116, 1983.

[54]. C. Tsang, K. Kwok, and P. Hitchcock, "Wind tunnel study of pedestrian level wind environment around tall buildings: Effects of building dimensions, separation and podium," *Building and Environment*, vol. 49, pp. 167–181, 2012.

[55]. K. T. Tse, A. U. Weerasuriya, Xuelin Zhang, S. W. Li, and K. C.S. Kwok, "Pedestrian-level wind environment around isolated buildings under the influence of twisted wind flows," *Journal of Wind Engineering and Industrial Aerodynamics*, vol. 162, pp. 12–23, 2017.

[56]. K. Deb, A. Pratap, S. Agarwal, and T. Meyarivan, "A fast and elitist multiobjective genetic algorithm: NSGA-II," *IEEE Transactions on Evolutionary Computation*, vol. 6, no. 2, pp. 182–197, 2002.

[57]. V. Srinivasan and A. D. Shocker, "Linear programming techniques for multidimensional analysis of preferences," *Psychometrika*, vol. 38, no. 3, pp. 337–369, 1973.

[58]. G. H. Tzeng and J.-J. Huang, *Multiple attribute decision making: methods and applications*. Boca Raton (Florida): CRC Press, 2011.

[59]. J. Guisado, F. Jiménez-Morales, and J. Guerra, "Application of shannons entropy to classify emergent behaviors in a simulation of laser dynamics," *Mathematical and Computer Modelling*, vol. 42, no. 7-8, pp. 847–854, 2005.

[60]. R. Yoshie, A. Mochida, Y. Tominaga, H. Kataoka, K. Harimoto, T. Nozu, and T. Shirasawa, "Cooperative project for CFD prediction of pedestrian wind environment in the Architectural Institute of Japan," *Journal of Wind Engineering and Industrial Aerodynamics*, vol. 95, no. 9-11, pp. 1551–1578, 2007.

[61]. X. Zhang, A.U. Weerasuriya, Bin Lu, K.T. Tse, Chun Ho Liu, and Y. Tamura, Pedestrian-level Wind Environment near a Super-Tall Building with Unconventional Configurations in a Regular Urban Area. *Building Simulation*, (DOI: 10.1007/s12273-019-0588-3), 2019.